THE ASTROPHYSICAL JOURNAL, 439:793–799, 1995 February 1

GRAINS IN IONIZED NEBULAE: SPECTRAL LINE DIAGNOSTICS

J. KINGDON,[1] G. J. FERLAND,[1] AND W. A. FEIBELMAN[2]
Received 1994 May 31; accepted 1994 August 9

ABSTRACT

The depletion of condensable elements onto grains in gaseous nebulae can provide evidence that dust is well mixed with the ionized gas. Al and Ca are two of the most depleted elements in the general interstellar medium, and it is therefore important to measure their abundances within the ionized region of nebulae. We compute a large grid of photoionization models and identify sets of line ratios which are relatively insensitive to stellar and nebular parameters, and are thus excellent diagnostics for determining relative abundances. Based on the absence of the [Ca II] $\lambda\lambda$7291, 7324 doublet and the detection of Al II] $\lambda\lambda$2660, 2669 in the ultraviolet, we determine the extent of aluminum and calcium depletion onto grains in NGC 7027 and the Orion Nebula. Our results show a $\sim$0.3 dex depletion for Al, but a depletion of more than two and a half orders of magnitude for Ca. A similar calculation based on Mg II λ2798 yields roughly a 0.8 dex depletion for Mg. This reaffirms the discrepancy between depletions determined from high and low ionization Mg lines. We also find evidence for a "depletion gradient" in Ca in NGC 7027, since the calcium depletion we infer for the outer, more neutral regions using [Ca II] is somewhat higher than that inferred for the inner high-ionization region, using [Ca V]. This gradient can test current models of the survival of grains within hot ionized gas.

Subject headings: dust, extinction — ISM: abundances — line: profiles

1. INTRODUCTION

Two of the most important questions in nebular studies are what amount of dust exists in gaseous nebulae, and where the dust is located. Although grains might be expected to survive for long periods in neutral, well-shielded regions, it is not known how long they survive in the more hostile ionized region (Draine & Salpeter 1979). The depletion of condensable elements onto grains provides indirect evidence for the existence of dust (see Gaskell, Shields, & Wampler 1981; Shields 1975). Therefore, by comparing the gas-phase abundances of these elements to solar or stellar values, an estimate of the amount of depletion onto grains can be made.

Al and Ca are strongly depleted in the interstellar medium (ISM). Turner (1991) gives average depletions of $\sim$1.5 and $\sim$2.5 dex, respectively. In the ISM, the gas-phase abundances are correlated with density (see Mathis 1990). Little is known about the depletion of these elements in nebulae. In the optical, Al has no strong spectral lines, while Ca has two weak lines due to [Ca V] at λ5309 and λ6087, the latter of which is sometimes blended with a line due to [Fe VII]. Based on [Ca V] $\lambda\lambda$5309, 6087, Shields et al. (1981) found a depletion of roughly one order of magnitude for this element in the PN NGC 2440. Similarly, Keyes, Aller, & Feibelman (1990, hereafter KAF) estimate a depletion of roughly a factor of 5 for NGC 7027 from the λ5309 intensity. Both of these are much smaller depletions than that found in the general ISM.

Pwa, Mo, & Pottasch (1984) and Pwa, Pottasch, & Mo (1986) were able to determine Al depletions in the PNs NGC 6543 and BD+30°3639 by making UV observations with the *International Ultraviolet Explorer* (*IUE*). Their technique consisted of measuring *absorption* lines from the central stars in these objects. Their results suggest an Al depletion of an order of magnitude for the latter nebula and an upper limit of two orders of magnitude for the former.

Here we predict emission-line intensities of several Al and Ca lines by incorporating these elements into the photoionization equilibrium code described by Ferland (1993). A brief discussion of our improvements to this code can be found in Appendix A. We produce a grid of nebular models spanning a wide range of hydrogen density and central star temperatures. We identify several line ratios which are insensitive to stellar or nebular parameters, but are sensitive to abundance ratios. These grids are then compared with observational data to determine depletions.

In § 2, we present observational data for Al and Ca in the well-studied planetary nebula NGC 7027, and for Ca in Orion. In § 3, we use these data combined with model results to determine estimates to the gas-phase Al and Ca abundances. Finally, we discuss our results in § 4.

2. OBSERVATIONAL DATA

2.1. Al *in NGC 7027*

In order to determine the amount of Al present in NGC 7027, we have used the *IUE* observations reported by Keenan et al. (1992). These authors made the first detection of the intercombination line Al II] $\lambda\lambda$2660, 2669. They obtain an observed flux of 6.6×10^{-14} ergs cm^{-2} s^{-1} for 2660 from LWR 2571, and a flux of 9.2×10^{-14} ergs cm^{-2} s^{-1} for 2669 from LWR 2571. The sum of these two lines relative to He II λ2511 (average flux of 1.6×10^{-13} ergs cm^{-2} s^{-1}) from the same exposure is $\sim$0.55, corrected for reddening using the extinction curve of Seaton (1979) and $C = 1.47$ (KAF). Then using the UV data of KAF, we derived a reddening-corrected intensity for the Al II] λ2665 doublet of $\sim$0.042 relative to the C II] λ2326 intercombination line by scaling to the He II line.

[1] Department of Physics and Astronomy, University of Kentucky, Lexington, KY 40506.
[2] Laboratory for Astronomy and Solar Physics, Code 684.1, NASA/Goddard Space Flight Center, Greenbelt, MD 20771.

The C II] multiplet is blended with [O III] λ2321. Since the intensity of the oxygen line should be 0.12 times that of [O III] λ4363 based on transition probabilities, we used the KAF intensity of this latter line to subtract the blend. The [O III] λ2331 line is $\sim 10^{-3}$ times smaller than 2321, so its contribution to the blend is negligible.

2.2. Ca

We show below that the calcium doublet [Ca II] $\lambda\lambda$7291, 7324 (^2S–^2D) is expected to be quite strong in nebulae for solar abundances. However, it is not strong in published spectra of either PNs or H II regions, even those done at high resolution or with long exposure times. We examine the implications of this fact in two objects below.

2.2.1. Ca *in NGC 7027*

We used the observations of KAF for NGC 7027. The [Ca II] doublet was not detected. This study involved detection of very weak features, and is thus well-suited for our calculations. We determined the detection limit of these observations by finding an appropriately weak line, and then considering this to be an upper limit to the $\lambda\lambda$7291, 7324 intensity. Our criteria for choosing the reference weak line were (1) that it be well-identified, to avoid the possibility of ghosts or spurious detections; and (2) that it be relatively close in wavelength to $\lambda\lambda$7291, 7324, to avoid problems with reddening and signal-to-noise. We chose the He I λ7500 line, which gives a reddening-corrected intensity of $\lambda 7500/\mathrm{H}\beta = 2.85 \times 10^{-4}$. We take this to be an upper limit to the intensity of [Ca II] $\lambda\lambda$7291, 7324. Similarly, with respect to the [S II] λ6720 doublet, we obtain $\lambda 7506/\lambda 6720 \leq 4.33 \times 10^{-3}$. We shall use these two limits to determine the Ca abundance in the next section.

2.2.2. Ca *in Orion*

We also consider the benchmark H II region the Orion nebula. Our observations were taken from Osterbrock, Tran, & Veilleux (1992), which include many faint lines. Again, the [Ca II] doublet feature was not observed. For our weak line, we used [Ni II] λ7412 which gave results analogous to that determined for NGC 7027 of $\lambda\lambda 7291, 7324/\mathrm{H}\beta \leq 2.70 \times 10^{-4}$ and $\lambda\lambda 7291, 7324/\lambda 6720 \leq 3.13 \times 10^{-3}$.

3. MODELS

In this section, we compute several grids of photoionization models in order to derive theoretical line intensity ratios for comparison with the observational data. We consider a gas ionized by a blackbody with a total luminosity of 10^{38} ergs s^{-1}. This luminosity is typical of a 1 $M_\odot$ PN nucleus at the Eddington limit, or of an O star. We show below that our results are not sensitive to the specific luminosity assumed. The assumed geometry is spherical, with an inner radius of 10^{17} cm. The results are not sensitive to the value of the inner radius. We have used a constant density throughout, with a filling factor of unity. We first consider solar abundances, taken from Grevesse & Anders (1989), and vary these abundances later. The total hydrogen density (n_H) and the temperature of the ionizing star (T_*) were varied. The range of density [$2.0 \leq \log (n_H) \leq 6.0$] was chosen to cover as wide a range of gaseous nebulae as possible (see Torres-Peimbert & Peimbert 1977; Barker 1978; Aller & Czyzak 1983; Aller & Keyes 1987). The low extreme of T_* comes from the coolest stars capable of producing an H II region (see Osterbrock 1989), while the high extreme is derived from the hottest measured PN central stars (Gathier & Pottasch 1989; Preite-Martinez et al. 1991). We then computed a grid of 778 models, using various combinations of the two variables.

In order to derive relative abundances, and thereby, depletions from spectral lines as accurately as possible, we must identify line ratios which are independent of nebular or stellar parameters. We examined many pairs of lines and identified several line ratios shown in Figure 1. We discuss each ratio and its implications below.

For Ca, we consider both [Ca II] $\lambda\lambda$7291, 7324/Hβ and [Ca II] $\lambda\lambda$7291, 7324/[S II] λ6720, shown in Figures 1*a* and 1*b*, respectively. These line ratios are not strongly sensitive to the assumed parameters. For instance, changes of 0.25 dex in n_H of and 0.2 dex in T_* result in changes in these ratios of 22% and 38%, respectively. These variations, and those quoted for our other line ratios, are average values obtained by examining several points equally spaced around the grid. In general, the dispersion at each point differs little from the average. As these chosen uncertainties in n_H and T_* are rather extreme, we expect the actual uncertainty in the Ca line ratios to be less than these values. Because sulphur is expected to be only mildly depleted (see Clegg 1989), a comparison between Figures 1*a* and 1*b* and the observations provides a direct indication of the Ca depletion. Using reasonable ranges of the parameters n_H and T_* for NGC 7027 ($\log n_H = 4.7$–4.85, $\log T_* = 5.24$–5.3; see KAF; Middlemass 1990; Gruenwald 1989) and Orion ($\log n_H = 3.6$–4.0, $\log T_* = 4.55$–4.6; see Rubin, Dufour, & Walters 1993; Osterbrock et al. 1992; Baldwin et al. 1991; Rubin et al. 1991), it is readily apparent by comparing the observed upper limits of the last section and Figures 1*a* and 1*b* that Ca is depleted by two to three orders of magnitude relative to solar in both NGC 7027 and Orion.

Figure 1*c* presents contour plots for the ratio Al II] λ2665/C II] λ2326. As is apparent from the figure, this ratio is remarkably insensitive to the assumed values of n_H and T_*. For the same range in n_H and T_* given for the Ca ratios, this ratio changes on average by $\sim$32%. We also note that, especially for the high T_* typical of PN central stars, the value of this ratio is almost completely independent of n_H. Since stellar temperatures are generally known to a better degree than nebular densities, this further strengthens the usefulness of the ratio. Comparing Figure 1*c* with the observations of the last section indicates that the Al/C abundance ratio is roughly a factor of 4 less than solar. In NGC 7027 C is increased relative to solar by roughly a factor of 2, so half of this depletion is due to selective C enhancement.

Another element whose depletion has been somewhat controversial is Mg. We find that the line ratio Mg II λ2798/C II] λ2326 is also relatively insensitive to n_H and T_*, with a value changing by an average of $\sim$40% for the above-mentioned range in these parameters. As depicted in Figure 1*d*, the behavior of this ratio is very similar to the Al/C line ratio, including the lack of n_H-dependence for large T_*.

The Mg II doublet is difficult to measure observationally, due to absorption by interstellar gas as well as destruction by internal dust. The importance of interstellar absorption of this line was discussed by Clegg et al. (1987), and was shown to be a function of the object's velocity with respect to the local standard of rest by Middlemass (1988). Middlemass demonstrated how it was possible to reconstruct the line intensity using high-resolution *IUE* spectra. In a model of NGC 7027 (Middlemass 1990), he determined that the intensity of this line should be increased by a factor of 1.83 to correct for ISM absorption. We have independently verified this result by reexamining the

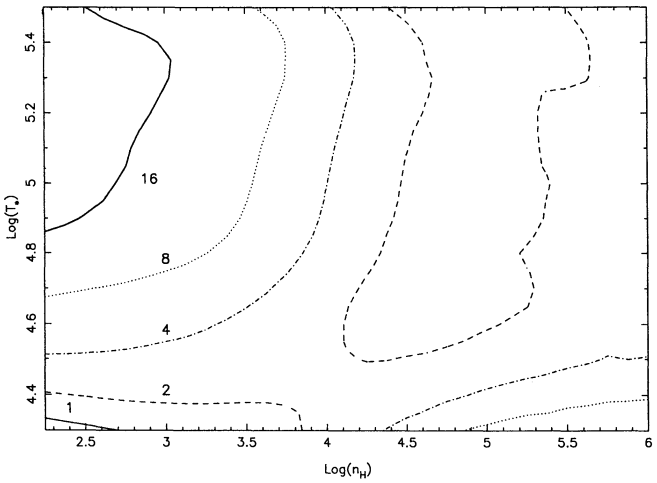

FIG. 1*a*

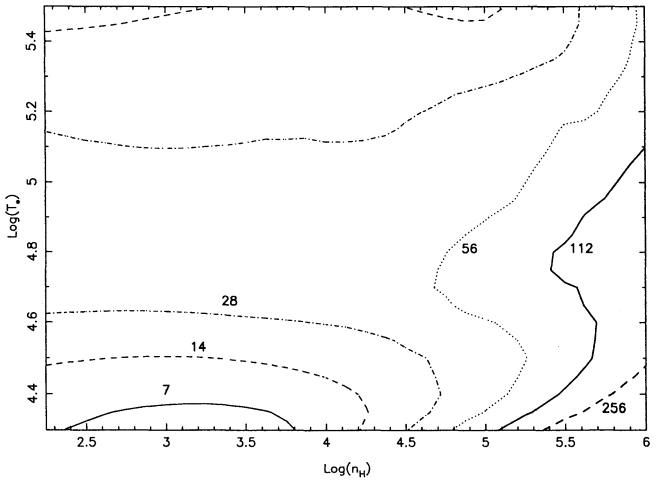

FIG. 1*b*

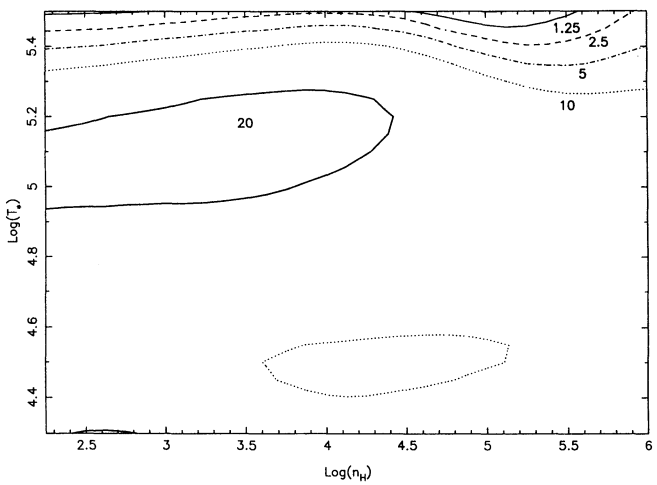

FIG. 1*c*

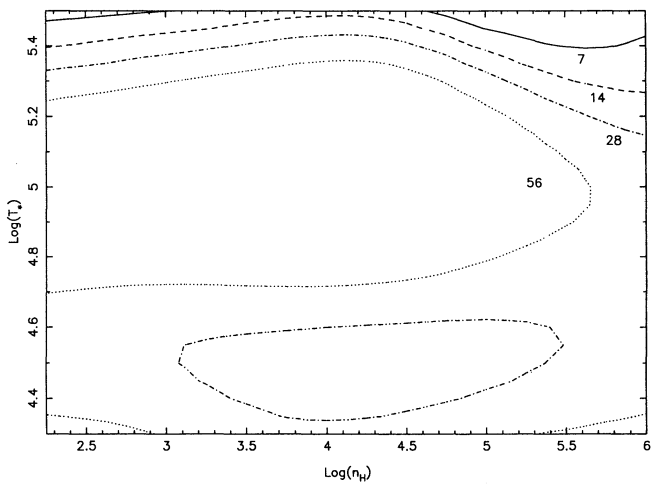

FIG. 1*d*

FIG. 1.—Contour plots of various line ratios as functions of central star temperature and total hydrogen density. The abundances are solar and grains are not included. The contours are multiplied by the following factors: (*a*) 10^2, (*b*) 10^2, (*c*) 10^2, (*d*) 10.

observational data. Clegg et al. (1987) have also determined that internal destruction by dust further weakens the line by a factor of 1.5–2.0. We discuss this latter effect below.

Using the observations of KAF and correcting for the ISM absorption as detailed above, we derive a relative intensity of Mg II λ2798/C II] λ2326 = 0.32. Comparison with Figure 1*d* suggests a Mg/C abundance ratio roughly 19 times smaller than solar. Again, roughly half of this is due to the enhanced C, so we are left with a depletion of roughly 1 dex. By comparison, Mg is depleted by roughly 0.5 dex in the ISM.

In order to quantify these results, we have computed a second grid of models. These are identical to the first set with two major exceptions. First, we have introduced grains into the calculations. We include both graphite and silicate grains with a dust-to-gas ratio equal to that of the ISM. We show below that our results are not sensitive to the assumed dust-to-gas ratio. The numerical simulation includes thermal and ionization/recombination processes, as described by Baldwin et al. (1991). Second, we used gas-phase abundances more typical of PNs, with the exception of C, Mg, and Al, which were left with solar abundances. As none of these elements produce strong coolants, their abundances should have little effect on our results. The abundances of the elements are listed in Table 1. We then varied the Ca abundance until a good match was made to both observed line ratios for both NGC 7027 and Orion.

Figure 2 shows the same line ratios as Figure 1, using the

TABLE 1

MODEL ABUNDANCES

Ratio	Solar (Grevesse & Anders 1989)	PN
He/H	0.098	0.10
C/H.....	3.63(−4)	3.63(−4)
N/H	1.12(−4)	1.8(−4)
O/H	8.51(−4)	4.4(−4)
Ne/H	1.23(−4)	1.1(−4)
Na/H	2.10(−6)	3.0(−7)
Mg/H.....	3.80(−5)	3.8(−5)
Al/H	2.95(−6)	2.95(−6)
Si/H	3.55(−5)	1.0(−5)
S/H	1.62(−5)	1.0(−5)
Ar/H.....	3.63(−6)	2.7(−6)
Ca/H	2.29(−6)	7.6(−9)
Fe/H.....	4.68(−5)	5.0(−7)
Ni/H.....	1.76(−6)	1.8(−8)

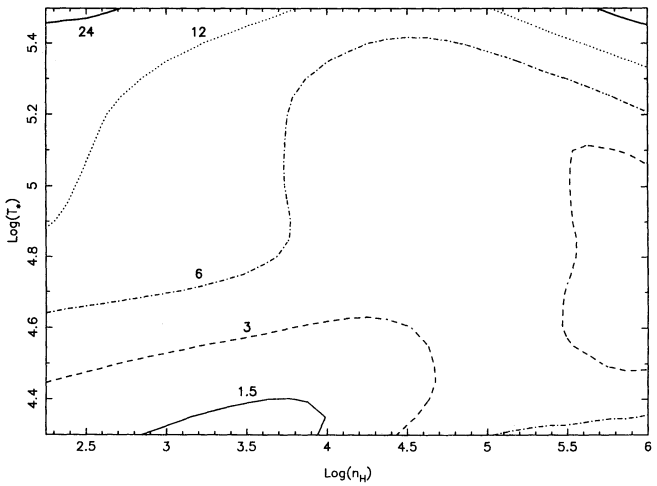

FIG. 2a

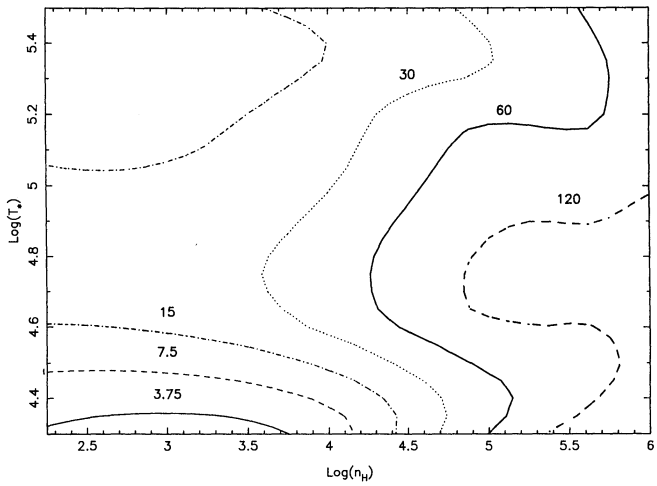

FIG. 2b

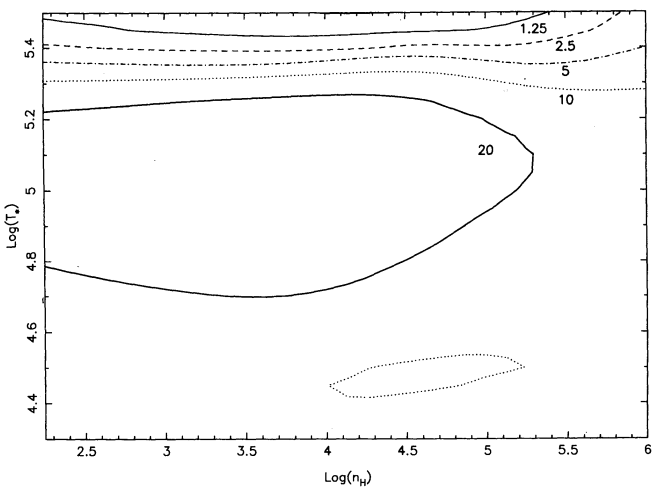

FIG. 2c

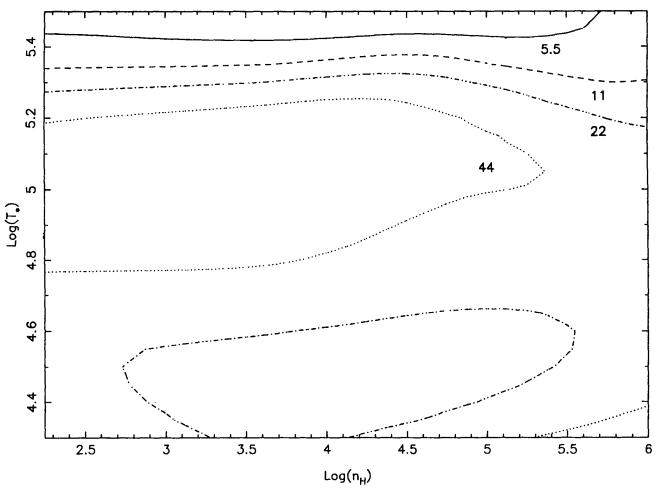

FIG. 2d

FIG. 2.—Contour plots of various line ratios as functions of central star temperature and total hydrogen density. The nonsolar abundances are listed in Table 1, and grains are included. The contours are multiplied by the following factors: (*a*) 10^4, (*b*) 10^4, (*c*) 10^2, (*d*) 10.

parameters from the second grid. Our results gave an upper limit of log (Ca/H) = −8.11 for Orion and a value of log (Ca/H) = −8.14 for NGC 7027. Both of these are roughly two and a half orders of magnitude below solar. The Al/C abundance ratio derived from Figure 2*c* is a factor of 4 less than solar, essentially unchanged from our initial calculations. Using the derived value C/H = 6.45×10^{-4}, for NGC 7027 from KAF, this yields an Al depletion of only a factor of ∼2.2.

As we will show in the next section, the main difference between Figure 1*d* and Figure 2*d* is the inclusion of grains and the resultant destruction of optically thick lines by continuous absorption. A comparison between the observed and predicted Mg/C line ratios yields a relative depletion for Mg/C of a factor of 10. Using the above value for the C abundance in NGC 7027 yields a Mg depletion of a factor of 6. This revised value is reduced from the 1 dex deduced previously due to the destruction of the Mg II λ2798 line by grains.

At this point, we wish to examine the effect of our chosen model parameters on the above results. As demonstrated in the last section, all of our chosen line ratios are only weakly dependent on the assumed values of n_H and T_*. For the Ca ratios especially, the variation is significantly less than the derived depletion.

Another uncertainty is our choice of abundances. The primary manner in which heavy elements affect the emission-line spectrum is through cooling via collisionally excited lines. A comparison between Table 1 and solar abundances shows that there is not a significant difference between the values of the major coolants. This, coupled with the small variation of our chosen line ratios with temperature, suggests that our assumed abundances will have little effect on the measured depletions. We verify this below.

The major effect of grain inclusion is also to modify the temperature within the nebula through photoelectric heating and collisional cooling. Our choice of a dust-to-gas ratio equal to the ISM was made based on the work of Mallik & Peimbert (1988). Again, due to the relative insensitivity of our line ratios to temperature, the inclusion of grains or the chosen dust-to-gas ratio does not significantly affect our results.

In order to quantify these expectations, we have conducted two tests. First, we ran several models with the same parameters and depleted Ca abundance as in our second grid, but

with the abundances of the other elements set to solar. Grains were not included. We then compared these results with those from another run using the nebular abundances and also without grains. This should determine the affect of abundances on our results. Second, we have rerun several models from our second grid, eliminating grains (i.e., using a dust-to-gas ratio of 0.0). We then compare these results with that of our second grid. This will measure the effect of grains. We discuss our results for each line ratio individually below.

We first discuss the Ca line ratios. Using the abundance comparison described above, we find that the change in abundances results in a difference of $\sim 20\%$ for Orion for Ca/H, and a difference of $\sim 40\%$ for Orion for Ca/S. For both line ratios, the effect on NGC 7027 was less than 15%. Including grains but leaving the gas-phase abundances fixed at the depleted values resulted in an increase of an average factor of ~ 2.5 for both ratios for Orion, and an increase of an average factor of ~ 5 for both ratios for NGC 7027. These changes are the results of the role that grains play in modifying the heating-cooling balance in the nebula, and as a continuous opacity source. Both the change to nebular abundances and the inclusion of grains have the effect of *increasing* the derived Ca depletions for Orion by the above amounts. For NGC 7027, the effect of adding grains increases the derived depletions, but the use of nebular abundances decreases the depletions. However, in both cases, as these factors are essentially negligible compared to the factor of $\sim 10^{2.5}$ Ca depletion, they will have no appreciable effect on our results.

Because the lines used in the Al/C line ratio have similar excitation potentials, the ratio will depend only weakly on electron temperature. We therefore except that neither a change in abundances (other than Al and C) nor the addition of grains will much alter the values obtained for this ratio. This is evident from a comparison of Figure 1*c* and Figure 2*c*. To be specific, we found that the variation in abundances produced a change in the Al/C line intensity of less than 10%, while the inclusion of grains caused a $\sim 30\%$ decrease in the line ratio.

At first glance, a comparison between Figure 1*d* and Figure 2*d* would suggest that the Mg/C line ratio is strongly dependent on abundances and grains. The main reason for the difference is the effects of destruction of the Mg II $\lambda 2798$ resonance line by grains in Figure 2. The effect of changing gas-phase abundances is only on the order of $\sim 3\%$, while the inclusion of grains decreases the line ratio by an average factor of 2.2. This latter value is in reasonably good agreement with the range 1.5–2.0 found by Clegg (1989).

Finally, we examine the effect of the central star luminosity (L_*) on our results. We ran a series of models identical to those of our second grid, except that the luminosity was reduced to 10^{36} ergs s^{-1}. With the exception of the Ca/H line ratio, which displays a fairly strong dependence on L_*, we found that all line ratios changed by less than 0.2 dex, and most by less than 0.1 dex over the 2.0 dex interval in L_* at fixed values of n_H and T_*. The Ca/H line ratio *increased* with decreasing luminosity. Thus, a smaller assumed L_* would have the effect of *increasing* our measured depletion. Since the Ca depletion was determined by the best fit to both the Ca/H and Ca/S line ratios, the luminosity-dependence of the Ca/H line ratio should not affect our results.

In addition to the above tests, we also have examined the effect on our results of using stellar atmospheres rather than blackbodies in our models. We ran models for several values of n_H using Kurucz (1979) model atmospheres with $T_* = 30{,}000$ K and 50,000 K with $L_* = 10^{38}$ ergs s^{-1}. We then compared our four line ratios to those obtained previously using blackbodies. For the Al/C ratio, the average difference was $\sim 10\%$, while the Mg/C ratio showed a higher change of $\sim 25\%$. The Ca/H and Ca/S ratios showed larger differences, with average changes of a factor of 1.5 and 2, respectively. We note that for the two Ca ratios, the differences were significantly smaller for the 50,000 K atmospheres. None of these changes would significantly affect the results given here. In fact, in most cases, use of the stellar atmospheres rather than blackbodies would actually *increase* the measured depletions.

The above discussion has shown that our inferred depletions are not dependent on the assumed nebular and stellar parameters. In addition, the contour plots of Figure 2 can be extremely useful for deriving depletions of Ca II, Al II, and Mg II for a wide range of gaseous nebulae. To facilitate this use, we present in Figure 3 a contour plot of the commonly used ionization parameter (defined as the ratio of photon to hydrogen densities) as a function of n_H and T_*. If one has a measurement of the ionization parameter for a particular object, one can then place it in n_H and T_* space for comparison with Figures 1 and 2.

4. DISCUSSION

The derived Al abundance determined in the last section for NGC 7027 is smaller by a factor of 5.3 than that obtained by Pwa et al. (1986) for the PN BD + 30°3639 by using interstellar absorption features in the UV. A determination of Fe depletion in NGC 7027 by Shields (1975) found that this element was depleted by roughly 2 dex, an amount similar to ISM values. Apparently, the grains which form in PN can be as efficient as the ISM in depleting Ca and Fe, but less efficient in depleting Al. This may provide a clue to the nature of the grains in PNs.

The one order of magnitude depletion of Mg measured here for NGC 7027 based on Mg II is significantly larger than the Mg depletion derived by either KAF or Middlemass (1990) based on higher ionization lines of Mg ([Mg IV] and [Mg V]). This is precisely the situation suggested for Mg by Péquignot & Stasinska (1980), who found a cosmic abundance of Mg in NGC 7027 based on [Mg V], but a depletion of roughly one order of magnitude based on Mg II. Similar results were

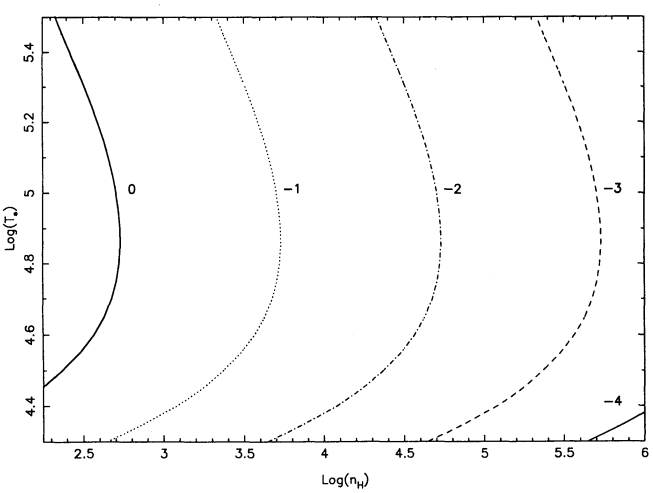

FIG. 3.—Contour plot of the log of the ionization parameter as a function of central star temperature and total hydrogen density.

obtained for Mg by Harrington & Marrioni (1981) for the PNs NGC 2165 and NGC 2440 and by Shields et al. (1981) for NGC 2440. Péquignot & Stasinska (1980) attributed their findings to a selective destruction of metallic magnesium grains by radiation heating during an early phase in the nebular expansion. We should note here, however, that these results for Mg have been weakened by two factors: (1) new collision strengths for [Mg v] from Mendoza & Zeippen (1987), which reduce the gradient, and (2) the previously mentioned interstellar absorption of the Mg II λ2800 line. Although both these factors reduce the measured gradient, models taking each into account (see Middlemass 1990) still find a gradient present.

Our Ca/H abundance ratio is depleted by three orders of magnitude from solar values. As shown in Appendix B, the [Ca II] emission occurs primarily near the outer edge of the H^+ zone. This clearly demonstrates not only that dust is present in gaseous nebulae, but more importantly, that it is mixed with the ionized gas. Rubin et al. (1993) reach a similar conclusion for Si in the Orion nebula. Our limits to the depletions for Ca are very similar to that found in the general ISM (see Turner 1991). However, estimates of the gas-phase abundance of Ca in PNs obtained from [Ca v] lines found depletions of only one order of magnitude, far less than the value determined here. These analyses relied on the intensity of [Ca v] λ5309, which is roughly a factor of 0.003 smaller than that of Hβ in NGC 7027 (KAF). This reference estimated an observational uncertainty of $\sim$20% for this line. It is also expected that since only one ionization stage of Ca was observed, the ICF will be quite large (for this particular reference, an ICF of 5.9 was used) and thus very uncertain. In addition, our inclusion of charge exchange will affect the relative amounts of each ion of Ca. We note here, however, that charge exchange does not directly affect λ5309, since the value of R_X for the line's upper level is significantly less than $7a_0$, and thus the rate coefficient is vanishingly small.

This suggests that Ca also possesses a depletion gradient, with the inner parts of the nebula, represented by [Ca v] having an essentially solar Ca abundance, while the outer zones, represented by [Ca II], show a strong depletion. This is analogous to the situation described above for Mg. For Ca, it is possible that spallation due to mass loss from the central star (see Draine & Salpeter 1979) would destroy dust grains in the inner regions of the nebula. Confirmation of these results for other nebulae would be useful, but difficult due to the aforementioned lack of strong Ca lines.

The authors wish to acknowledge informative discussions with A. Dalgarno and G. Lafyatis on the subject of charge exchange, and the useful suggestions of the referee, G. A. Shields. We acknowledge the support of NASA and NSF.

APPENDIX A

In this appendix, we discuss the basic atomic parameters used in our photoionization code, with particular emphasis on the newly derived charge transfer rate coefficients.

The Cloudy photoionization code simultaneously solves the equations of statistical and thermal equilibrium. Photoionization cross sections are taken from Reilman & Manson (1979) and radiative recombination coefficients from Aldrovandi & Péquignot (1974). We have included Al and Ca charge exchange rate coefficients which are discussed below.

We present new Landau-Zener (L-Z) charge exchange rate coefficients for reactions of the type $X^{+n} + H \rightarrow X^{+(n-1)} + H^+$, where X = Al or Ca, and $n > 1$. Although the L-Z method has theoretical limitations, it is usually sufficiently accurate for astrophysical applications. We use the expressions from Butler & Dalgarno (1980) for the incoming and outgoing channels, as well as their asymptotic form of the potential curve separation. The reader is referred to this reference for a more detailed account. Energy level wavenumbers were taken from Bashkin & Stoner (1975) or Moore (1949) for Al, and from Sugar & Corliss (1985) for Ca. We ignored fine structure and polarizability of the H core. The final rate coefficients were derived using the software by Bienstock (1983). In all calculations we have assumed the nebular approximation, i.e., both of the reactant ions are in their ground states.

In Table A1, we list the rate coefficients (in units of $cm^3\ s^{-1}$) for a range of temperatures. The results for Al^{+2} and Al^{+3} show that charge transfer with H is generally negligible for these ions. However, in these cases, charge transfer may occur by emission of a photon, i.e., $X^{+n} + H \rightarrow X^{+(n+1)} + H^+ + h\nu$. Rate coefficients for this radiative charge transfer are generally about 1×10^{-14} (Dalgarno 1978). The results for Al^{+4} were complicated by the lack of L-S coupling schemes for some levels, which prevented accurate determination of p_0. Likewise, for Al^{+5}, wavenumbers were not available for some levels. In the situation where several exit channels for a reaction have the same symmetry, simply summing the individual rate coefficients can lead to an overestimate of the total result. This is the case for Al^{+4} and Ca^{+4}.

TABLE A1

RATE COEFFICIENTS ($cm^3\ s^{-1}$)

Ion	10^3 K	$10^{3.5}$ K	10^4 K	$10^{4.5}$ K
[a] $Al^{+2} + H \rightarrow Al^+ + H^+$	1.00(−14)	1.00(−14)	1.00(−14)	1.00(−14)
[a] $Al^{+3} + H \rightarrow Al^{+2} + H^+$	1.00(−14)	1.00(−14)	7.11(−14)	8.18(−12)
[b,c] $Al^{+4} + H \rightarrow Al^{+3} + H^+$	5.76(−10)	6.30(−10)	7.68(−10)	1.83(−9)
[d] $Al^{+5} + H \rightarrow Al^{+4} + H^+$	5.43(−10)	7.50(−10)	9.97(−10)	1.80(−9)
$Ca^{+3} + H \rightarrow Ca^{+2} + H^+$	3.85(−12)	3.18(−11)	2.88(−10)	1.61(−9)
[c] $Ca^{+4} + H \rightarrow Ca^{+3} + H^+$	3.09(−10)	1.01(−9)	2.66(−9)	5.94(−9)
$Ca^{+5} + H \rightarrow Ca^{+4} + H^+$	9.71(−11)	1.00(−10)	1.03(−10)	1.04(−10)

[a] Radiative charge transfer rates have been set equal to 1.00(−14).
[b] Results are less accurate due to lack of L-S coupling schemes for some levels.
[c] Rates may be overestimated due to several channels having the same symmetry.
[d] Results are less accurate due to lack of wavenumbers for some levels.

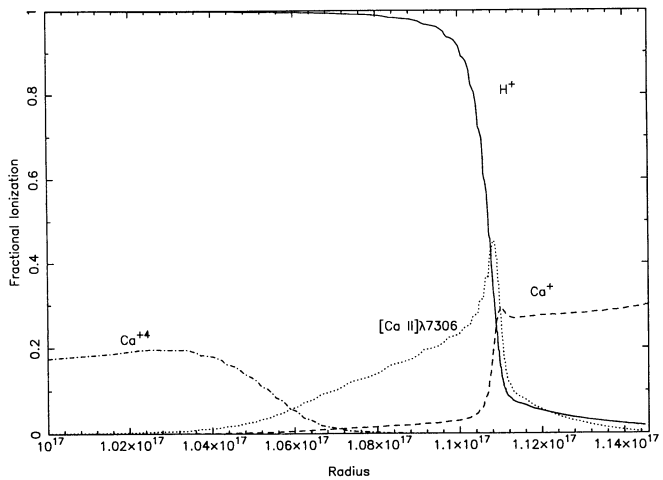

FIG. 4.—Fractional ionization vs. radius for model described in text. Solid line represents H^+, dashed line Ca^+, and dot-dashed line Ca^{+4}. The local emissivity of the [Ca II] λ7306 line is also plotted in arbitrary units (*dotted line*).

APPENDIX B

In this appendix, we demonstrate that the bulk of the [Ca II] λλ7291, 7324 emission occurs near the outer edge of the H^+ zone. This implies that the depletion measured from these lines occurs within the ionized zone as well.

We computed a model with the same parameters as that from our second grid, and with log (n_H) = 4.75 and log (T_*) = 5.27. The code's treatment of Ca is discussed in Ferland & Persson (1989). In Figure 4, we plot the fractional ionization of H^+, (*solid line*) Ca^+ (*dashed line*), and Ca^{+4} (*dot-dashed line*) as a function of nebular radius . Due to the low ionization potential of Ca^0, the Ca^+ zone extends far beyond the H^+ Strömgren radius. However, the emission of [Ca II] λλ7291, 7324 is weighted by the Boltzmann factor for excitation. Figure 4 also shows the local emissivity of this line (in arbitrary units) as a function of nebular radius (*dotted line*). It can be seen that the bulk of the emission occurs just within the H^+ zone. The sudden drop in the line intensity at the ionization front is a combination of a drop in the electron temperature as reflected in the Boltzmann factor, and a drop in the electron density.

REFERENCES

Aldrovandi, S., & Péquignot, D. 1974, Rev. Brasileira Fis., 4, 491
Aller, L. H., & Czyzak, S. J. 1983, ApJS, 51, 211
Aller, L. H., & Keyes, C. D. 1987, ApJS, 65, 405
Baldwin, J. A., Ferland, G. J., Martin, P. G., Corbin, M. R., Cota, S. A., Peterson, B. M., & Slettebak, A. 1991, ApJ, 374, 580
Barker, T. 1978, ApJ, 219, 914
Bashkin, S., & Stoner, J. O. 1975, Atomic Energy Levels and Grotian Diagrams (Amsterdam: North-Holland)
Bienstock, S. 1983, Comput. Phys. Comm., 29, 333
Butler, S. E., & Dalgarno, A. 1980, ApJ, 241, 838
Clegg, R. E. S. 1989, in IAU Symp. 131, Planetary Nebulae, ed. S. Torres-Peimbert (Dordrecht: Reidel), 139
Clegg, R. E. S., Harrington, J. P., Barlow, M. J., & Walsh, J. R. 1987, ApJ, 314, 551
Dalgarno, A. 1978, Planetary Nebulae, Observations and Theory, ed. Y. Terzian (Dordrecht: Reidel), 139
Draine, B. T., & Salpeter, E. E. 1979, ApJ, 231, 438
Ferland, G. J. 1993, Hazy, Univ. Kentucky Int. Rep.
Ferland, G. J., & Persson, S. E. 1989, ApJ, 347, 656
Gaskell, C. M., Shields, G. A., & Wampler, E. J. 1981, ApJ, 249, 443
Gathier, R., & Pottasch, S. R. 1989, A&A, 209, 369
Grevesse, N., & Anders, E. 1989, in AIP Conf. Proc. 183, Cosmic Abundances of Matter, ed. C. J. Waddington (San Francisco: AIP), 1
Gruenwald, R. B. 1989, in IAU Symp. 131, Planetary Nebulae, ed. S. Torres-Peimbert (Dordrecht: Reidel), 224
Harrington, J. P., & Marrioni, P. A. 1981, in The Universe at Ultraviolet Wavelengths (NASA CP 2171), 623
Keenan, F. P., Harra, L. K., Aggarwal, K. M., & Feibelman, W. A. 1992, ApJ, 385, 375
Keyes, C. D., Aller, L. H., & Feibelman, W. A. 1990, PASP, 102, 59 (KAF)
Kurucz, R. L. 1979, ApJS, 40, 1
Mallik, D. C. V., & Peimbert, M. 1988, Rev. Mexicana Astron. Af., 16, 111
Mathis, J. S. 1990, ARA&A, 28, 37
Mendoza, C., & Zeippen, C. J. 1987, MNRAS, 224, 7P
Middlemass, D. 1988, MNRAS, 231, 1025
———. 1990, MNRAS, 244, 294
Moore, C. E. 1949, Atomic Energy Levels, NBS Circ. 467
Osterbrock, D. E. 1989, Astrophysics of Gaseous Nebulae and Active Galactic Nuclei (Mill Valley: University Science Books)
Osterbrock, D. E., Tran, H. D., & Veilleux, S. 1992, ApJ, 389, 305
Péquignot, D., & Stasinska, G. 1980, A&A, 81, 121
Preite-Martinez, A., Acker, A., Köppen, J., & Stenholm, B. 1991, A&AS, 88, 121
Pwa, T. H., Mo, J. E., & Pottasch, S. R. 1984, A&A, 139, L1
Pwa, T. H., Pottasch, S. R., & Mo, J. E. 1986, A&A, 164, 184
Reilman, R. F., & Manson, S. T. 1979, ApJS, 40, 815
Rubin, R. H., Dufour, R. J., & Walter, D. K. 1993, ApJ, 413, 242
Rubin, R. H., Simpson, J. P., Haas, M. R., & Erickson, E. F. 1991, ApJ, 374, 564
Seaton, M. J. 1979, MNRAS, 187, 785
Shields, G. A. 1975, ApJ, 195, 475
Shields, G. A., Aller, L. H., Keyes, C. D., & Czyzak, S. J. 1981, ApJ, 248, 569
Sugar, J., & Corliss, C. 1985, J. Phys. Chem. Ref. Data, 14, suppl. 2
Torres-Peimbert, S., & Peimbert, M. 1977, Rev. Mexicana Astron. Af., 2, 181
Turner, B. E. 1991, ApJ, 376, 573